Structure and properties of (Na0.5Bi0.5)ZrO3 (NBZ) lead-free perovskite compound

Jerome Lelievre, Michaël Josse, Pascal Marchet

Structure and properties of $(Na_{0.5}Bi_{0.5})ZrO_3$ (NBZ) lead-free perovskite compound

Jerome Lelievre[1, 2], M. Josse[3] and Pascal Marchet[1,*]

[1] Université de Limoges, IRCER, UMR 7315, Limoges F-87068, France
[2] Present address: CTTC, Limoges F-87068, France
3. CNRS, Univ. Bordeaux, ICMCB, UMR 5026, F-33600 Pessac, France

* Corresponding Author.
E-mail address: pascal.marchet@unilim.fr

Abstract
The structure of NBZ was studied by neutron diffraction. NBZ is monoclinic, (SG #11 $P2_1/m$) a_m = 5.696(8) Å, b_m = 8.166(9) Å, c_m = 5.790(4) Å and β_m = 89.97(4)°. Being centrosymmetric, NBZ is neither piezoelectric nor ferroelectric. No phase transition was evidenced between 100 K and 923 K. NBZ presents a relaxor behavior below room temperature attributed to the mixed occupancy of the A-site by both Na^+ and Bi^{3+} ions. The relative permittivity of NBZ appears noticeably stable (for 1 kHz -2.9% at -55 °C / 218K and +5.3% at 85 °C / 358 K compared to the 25 °C / 298 K value). NBZ appears thus as promising for the elaboration of capacitors requiring high thermal stability.

Keywords
Lead-free perovskite; neutron diffraction; crystal structure; dielectric; relaxor

Currently, most of piezoelectric devices are using PZT, a lead-based solid solution of formula $Pb(Zr_{1-x}Ti_x)O_3$. Indeed, PZT-based compositions are the dominant piezoceramics due to their high electromechanical properties and low cost. Because of restrictions about the use of lead-based materials related to health and environmental problems, a huge scientific effort started about 20 years ago in order to substitute PZT. Nowadays, only a few lead-free materials are considered as possible candidates to this substitution and most of them are of perovskite structure: (i) $BaTiO_3$-based materials, (ii) Alkaline-niobates such as $(K,Na)NbO_3$ (KNN) and (iii) alkaline-bismuth titanates like $(Na_{0.5}Bi_{0.5})TiO_3$ (NBT) or $(K_{0.5}Bi_{0.5})TiO_3$ (KBT) [1-10]. Nevertheless, the search for new lead-free compounds is still topical question, whether or not this compounds are ferroelectric/piezoelectric. In addition, perovskite compounds presenting mixed occupancy of A or B-site (e.g. NBT or PMN) could also present relaxor behavior and interesting dielectric properties.

In the case of titanates, the possibility of substituting titanium by zirconium was evidenced a long time ago. Indeed, $PbTiO_3$, $PbZrO_3$, $BaTiO_3$ and $BaZrO_3$ are perovskite compounds, even if their structure and space groups are different. Thus, this replacement is probably also possible in complex perovskite compound like NBT. Surprisingly, this possibility has only been barely considered. After the discovery of NBT in 1961, Smolenskii considered the possible occurrence of the $(Na_{0.5}Bi_{0.5})ZrO_3$ (NBZ) compound but reported only dielectric measurement without any XRD pattern [11]. In 1995, a letter devoted to the dielectric properties of NBT-NBZ-KBT-KBZ system suggested the occurrence of NBZ as a “not identified” compound [12]. It was not until 2007 that NBZ was evidenced for the first time and its XRD pattern reported [13, 14]. NBZ was assigned to an orthorhombic structure (a = 4.379 Å, b= 7.489 Å and c = 7.078 Å), but the possible space group was not considered. The dielectric

properties and conduction mechanisms were also studied, evidencing a grain boundary effect around 350°C (623 K), associated to non-Debye type dielectric relaxation [13, 14]. A broad ferroelectric-paraelectric phase transition (diffuse phase transition) was reported at 425°C (698 K) [13]. The elaboration of NBZ powders and the densification mechanism of ceramics were studied and the orthorhombic space group Pnma (SG #62) was attributed to NBZ without any structural study [15, 16]. Ferroelectric properties were reported for NBZ [17], but: (i) this property is conflicting with the centrosymmetric Pnma space group and (ii) the elliptic shape of hysteresis loop is typical of a lossy dielectric and not of a ferroelectric material [18]. The evolution of lattice parameters and dielectric properties in the $(Na_{0.5}Bi_{0.5})(Zr_{1-x}Ti_x)O_3$ solid-solution were later studied [19-22], confirming that zirconium can totally substitute titanium in such complex perovskites, like for KBT-KBZ system [23]. To summarize: (i) the existence of the NBZ perovskite compound is clearly established, (ii) the reported space group and ferroelectricity are questionable, (ii) the occurrence of phase transitions is questionable. Therefore, the aim of the present study is: (i) to determine the structure of NBZ, (ii) to study the dielectric properties for a large temperature range including low temperatures and (iii) to try to detect possible phase transitions below and above room temperature.

The NBZ compound was firstly synthetized in alumina crucible using Na_2CO_3 (Aldrich 99+ %), Bi_2O_3 (Puretech 99.975 %) and ZrO_2 (Alfa Aesar, 99.7 %). A perovskite compound was obtained and XRD results evidenced a pattern similar to the one already reported [13-14]. Some secondary phases were also observed and assigned to Na_2ZrO_3, unreacted ZrO_2.and eventually to doped bismuth oxide such as $Na_{0.29}Bi_{1.71}O_{2.71}$. Similar result was obtained in platinum crucible thus excluding chemical reaction with crucible. Attempts to suppress this secondary phases by annealing were unsuccessful. As a consequence, the NBZ compound was finally synthetized by solid-state route using $NaBiO_3$ (Alfa Aesar, 80 %) and ZrO_2 (Alfa Aesar, 99.7 %). The raw materials were dried at 150 °C, weighted in stoichiometric amounts and calcined at 800 °C for 4 hours in alumina crucible. The weight losses associated to the volatilization of Na or Bi were checked as lower than 0.5 %. The XRD patterns ($\theta/2\theta$ diffractometer, D8 Panalytical, Cu $K_{\alpha 1}$) of the obtained powder evidenced less secondary phases than for preliminary synthesis. (see supplementary materials, fig. S1). The crystallographic study of the powders has been led by using neutron diffraction (Leon Brillouin Laboratory, 3T2 diffractometer, Saclay, France). The powder (≈ 10g) has been placed in a vanadium can and the diffraction data has been collected between 4.5 and 121° at 20 °C (293 K) during 8 hours at a 1.2289 Å wavelength for incident neutrons. Structural refinements were performed using the Jana 2006 software [24]. A mixture of plasticizer and binder (polyethylene glycol and polyvinyl alcohol) was added to the powder in order to obtain suitable green pellets, then shaped by uniaxial pressing (250 MPa, 10 mm diameter matrix). Sintering has been carried out at 900 °C / 4hours. Dielectric measurements were performed between 80 K and 450 K using an impedance analyzer (HP 4194A, 100Hz – 1MHz). Differential Scanning Calorimetry was performed on powders between 100 K and 350 K in order to search for phase transitions (DSC Q1000, TA Instruments) and by TG/DSC between 303 K and 1773 K (Netzsch STA 449F3). High temperature X-ray diffraction (HT-XRD) was performed between 300 K and 923 K in order to search for high temperature phase transitions.

As previously reported, powder neutron diffraction patterns (PND) evidenced that: (i) secondary phases Na_2ZrO_3 [25] and unreacted ZrO_2 [26] are observed, (ii) the main peaks of the perovskite structure are clearly split and (iii) some extra peaks are observed, indicating a superstructure due to octahedra tilting [27-30]. Another unidentified compound is also observed by XRD, probably coming from Na or Zr -doped bismuth oxide like $Na_{0.29}Bi_{1.71}O_{2.71}$, $Bi_{7.38}Zr_{0.62}O_{12.31}$ or $Bi_{7.38}Na_{0.62}O_{11.38}$. Considering the splitting of the main diffraction peaks of

the perovskite phase, the structure could be either orthorhombic, monoclinic or triclinic. Thus, the structural investigation was undertaken based on the group / subgroup relationships associated to the different possible tilt systems and taking into account the Na_2ZrO_3 and ZrO_2 secondary phases. The preliminary refinements quickly indicated a three tilts system, thus with possible space groups Pnma, C2/c, $P\bar{1}$ or $P2_1/m$ [31]. The former three groups gave results with quite poor quality factors or did not converge.

Refinement using the monoclinic $P2_1/m$ were then performed, using as starting parameters the atomic positions of the $ScRhO_3$ compound [32]. After refinement of the atomic positions, isotropic displacement parameters were refined. In a third step, anisotropic parameters for the (Na^+/Bi^{3+}) pseudo-ion improved the results (see supplementary material, table 1), while the use of anisotropic parameters for other ions gave a non-meaningful solution. Therefore, anisotropy was only retained for (Na^+/Bi^{3+}) pseudo-ion. The observed, calculated and difference curves for the final refinement are represented in fig. 1. The profile fit quality factors are satisfactory (Rp = 2.66%, wRp = 3.53%), indicating that the refinement with this space group is adequate.

As for all perovskite compounds, the structure corresponds to a network of tilted corner-sharing [ZrO_6] octahedra (fig. 1 b & c). The octahedra are tilted along the three directions, with a tilt system $a^-a^+c^-$ in Glazer notation (i.e. tilt system #9 [27]). Two kinds of octahedra are encountered, forming in phase tilted chains along the [010] direction and linked by O(3) and O(4). The first type includes Zr(1), O(2), O(3) and O(4) while the second one includes Zr(2), O(1), O(3) and O(4). These ZrO_6 octahedra are slightly distorted with three different Zr-O distances. However, this distortion is small and these distances remains close to the mean value of 2.099 Å, with angles close to 90° (see supplementary material, table 1 and fig S2). The situation is different for the (Na^+/Bi^{3+}) pseudo-ion. For sake of accommodation of (Na^+/Bi^{3+}) pseudo ion, and the lone pair of the latter, the cuboctahedral 12 fold coordinated cavity is turned into an 8-fold coordinated polyhedron by means of octahedra tilting, with several bond lengths between 2.41 and 2.97 Å. Moreover, the (Na^+/Bi^{3+}) pseudo-ion is represented by a flattened ellipsoid. These flattened ellipsoids have their larger directions in planes which are approximately {110} planes of the primitive perovskite cell forming 90 ° angles for the (Bi_1/Na_1) and (Bi_2/Na_2) sites. This effect probably comes from both compositional (Na/Bi) and spatial (different Na/Bi polyhedra) disorder on the A-site of the perovskite lattice induced by the mixed occupancy by two different ions, to which the lone-pair stereochemistry of Bi is adding. The chemical formula obtained by the refinement, $(Na_{0.46}Bi_{0.54})ZrO_3$, is only slightly different from the initial value $(Na_{0.5}Bi_{0.5})ZrO_3$. However, the chemical composition, calculated by using the mass fraction obtained by the refinement, indicates a Na/Bi ratio 0.61:0.44. This bismuth deficiency is probably due to its volatilization during synthesis, as frequently observed for other Bi-containing compounds. Furthermore, it must be noticed a trend to Na^+ and Bi^{3+} ordering between the [Bi_1/Na_1] and [Bi_2/Na_2] sites: the [Bi_1/Na_1] ratio is 0.124:0.376 and 0.416:0.084 for [Bi_2/Na_2], against 0.5:0.5 initial value. This results indicates a tendency to Na enrichment for the first site and to the reverse for second one. Such Na/Bi ordering was reported in the homologous compound NBT [33-35]. Thus this phenomenon is not only observed in the case of NBZ. This ordering is correlated with mean displacement of (Na/Bi) ions since the direction of these displacements is different for the (Bi_1/Na_1) site which is Na rich and (Bi_2/Na_2) site which is Bi rich. Finally, these results clearly demonstrate that the correct space group of NBZ is $P2_1/m$ and that the previous assignment to Pnma space group was unsuitable. As a consequence, and since this space group is centrosymmetric, NBZ can't be neither a ferroelectric nor a piezoelectric compound.

The XRD pattern of the studied ceramic pellet evidenced unreacted ZrO_2.secondary phase and that Na_2ZrO_3 was eliminated during sintering (see supplementary materials fig. S1). However and because of the mixed occupancy of the A-site of the perovskite lattice by both Bi and Na-ions, some relaxor properties could be eventually observed. As a consequence, the relative permittivity ε' and dielectric losses tan(δ) of NBZ were investigated between 80 K and 450 K using frequencies ranging from 100 Hz to 1 MHz (Fig. 2). Higher temperatures were not investigated because of low densification of the sample. Several anomalies are observed: (i) between 100 K and 200 K, ε' is dependent on frequency and associated to a peak of tan(δ), (ii) from 250 K to ≈ 400 K, the relative permittivity remains quasi constant, (iii) above 400 K, ε' and tan(δ) increase quickly.

Between 100 K and 200 K, ε' is dependent on frequency and associated to a peak of tan(δ). This phenomenon is thus clearly associated to a relaxation process, as for the relaxor part of solid-solutions like $BaTiO_3$-$BiScO_3$ or $BaTiO_3$-$Bi(Zn_{2/3}Nb_{1/3})O_3$, for which the chemical disorder in A-site or B-site of the perovskite lattice disrupts the long range ferroelectric order and changes the behavior to relaxor [36-38]. In the case of NBZ, this relaxation phenomena is probably related to the partial chemical ordering observed on the (Na/Bi) sites. The lack of epsilon peak is probably associated to the low temperature of the freezing of polar nano regions associated to local ordering. The relaxation phenomena are generally analyzed using the temperature t_m of the maximum of the permittivity peak, which also corresponds to the inflexion point of the peak of tan(δ) curve. Since ε' doesn't present any maximum, the relaxation phenomena was analyzed using the temperature t_m of the inflexion point of the tan(δ) curve for a given frequency (see supplementary materials, fig. S3). Both Arrhenius and Vogel-Fulcher fits to the frequency dispersion were considered [36]: $f = f_0 e^{-\frac{E_a}{k_b T_m}}$ for Arrhenius and $f = f_0 e^{-\frac{E_a}{k_b (T_m - T_f)}}$ for Vogel-Fulcher, where f is the frequency associated to the temperature T_m of the inflexion point of the tan(δ) curve, f_0 the attempt jump frequency, E_a the activation energy, k_b the Boltzmann constant and T_f the freezing temperature. (see supplementary materials fig. S4 for the results of the fit). For both cases, the correlation coefficient is close to unity indicating a good fit of the data (R^2 = 0.997 and 0.996). However, the attempt jump frequency obtained for Arrhenius fitting (f_0 = 1.6 10^{15} Hz) seems quite large compared to reported values (5.10^9 to 9.10^{12} Hz) [36]. The Vogel-Fulcher fit considers dipole dynamic initiated above a freezing temperature, T_f, thus similar to dipolar glasses. This model is generally more appropriate for dielectric relaxors and T_f is the temperature below which thermal energy is no longer sufficient to permit dipolar cluster dynamics in relaxors [36]. The obtained results for the VF model (E_a = 0.17 eV, f_0 = 6.8 10^{11} Hz) are very similar to the one obtained for the $BaTiO_3$-$BiScO_3$ or $BaTiO_3$-$Bi(Zn_{2/3}Nb_{1/3})O_3$ systems (E_a = 0.24 – 0.26 eV, f_0 = 10^{11} - 10^{12} Hz) [36-38]. For the $BaTiO_3$-$BiScO_3$ system, this behavior, which also implies a similar trend of the dielectric properties, was attributed to a dipolar glass behavior associated to non-interacting or weakly coupled polar nanoregions [37]. In our case, similar phenomena could be due to the mixed occupancy of the A-site of the perovskite lattice by both Na^+ and Bi^{3+} ions.

Above the relaxation range and between 250 K and ≈ 400 K, the relative permittivity remains quasi constant and the relative permittivity depends very few on frequency. At 300 K ε_r = 73.3 for 100 Hz, 84.1 for 1 kHz, 83.7 for 10 kHz, ε_r = 83.3 for 100 kHz and 82.7 for 1 MHz. This material appears thus as very suitable for dielectric applications, for which frequency stability is required. In additions, the thermal evolution is very limited: the relative change of ε' (using the EIA standard for temperatures) $\Delta C = \frac{C - C_0}{C_0}$ at 1 kHz is -2.9% at -55 °C / 218K and

+5.3% at 85 °C / 358 K compared to the 25 °C / 298 K value. The low values of the dielectric constant seems to confirm the absence of polar order, contrary to the parent compound $(Na_{0.5}Bi_{0.5})TiO_3$ (NBT) for which a long range ferroelectric order is observed, associated to high relative permittivity ($\varepsilon_r \approx 500$ at 300 K [39]).

The increase of ε' and tan(δ) above 400 K corresponds to the increasing conductivity of the material. Indeed, previous studies reported a hopping conduction mechanism associated to bismuth volatilization during sintering [13-14]. Such mechanism induces oxygen vacancies which increase conductivity of the material and the dielectric losses. However, this phenomenon appears at a lower temperature (around 400 K) than previously reported (around 300 °C i.e. 573 K) [14]. This difference could be due to the sintering process. Indeed, previous reports concern ceramic samples sintered under oxygen, while our samples were sintered in air. Therefore, oxygen losses are probably larger in our case and the hopping conductivity mechanism is thus triggered at a lower temperature.

Concerning the polar properties, since the crystal structure is described in the centrosymmetric $P2_1/m$ space group from 100 K to 900 K, the NBZ compound can present neither piezoelectricity nor ferroelectricity in this temperature range. Therefore, the previous assignment of ferroelectric properties for NBZ was incorrect [17]. Attempts to detect electrostrictive properties were unsuccessful. Furthermore, and since NBZ is not cubic and presents a three tilts system, one can suppose that phase transitions towards other symmetries could exist for this compound (change of tilt system and/or change of crystalline symmetry). Therefore, we investigated for such phase transitions by DSC (low temperature range) and TG/DSC and HT-XRD above room temperature (see supplementary materials fig. S5-7). Below room temperature, we didn't detect any phase transition by DSC. The absence of thermal event in the DSC results confirms that the low temperature anomaly of the dielectric constant comes only from a relaxation process, without any associated phase transition.

Above room temperature, apart from water desorption (330 K - 400 K), a jump of the baseline is observed in the range 615 K – 670 K (342-397°C). This event could be associated to a second order phase transition like the diffuse phase transition reported in the literature around 698 K (425° C) [13]. However, this event can't correspond to ferroelectric – paraelectric phase transition as previously reported [13], since the room temperature structure is non ferroelectric. Above room temperature, the HTXRD results only indicates a monotonous decrease of the monoclinic angle from $\beta = 90.04(7)°$ at 303 K (30 °C) toward $\beta = 90.03(6)°$ at 923 K (650 °C, fig. 3, standard deviation 0.002°). However, the phase transition reported at 698 K (425 °C) [13] was not detected and the splitting of the main peaks of the perovskite lattice persist. As a consequence and according to the group – subgroup relationships known for tilted perovskites [29], this event could correspond to a modification of tilt system (second order phase transitions) leading from $P2_1/m$ (a^-a^+c tilt system) to C2/m ($a^0b^-c^-$) or C2/c ($a^-b^-b^-$) monoclinic space groups.

A third thermal event associated to weight loss (1 %) was also detected between 840 K and 1000 K (567 °C – 727 °C). Because of weight loss, this event is probably associated to decomposition of the sample. Further investigation will be performed later in order to identify the existing phases for this temperature range. Finally, melting occurs at 1290 K (1017°C) associated to evaporation of liquid phase with a large weight loss (27.8%).

To sum up, the structure of NBZ was studied by neutron diffraction. The NBZ compound is monoclinic, with space group $P2_1/m$ (SG #11) and lattice parameters $a_m = 5.696(8)$ Å, $b_m = 8.166(9)$ Å, $c_m = 5.790(4)$ Å and $\beta = 89.97(4)°$. Since this space group is centrosymmetric, NBZ can present neither piezoelectric nor ferroelectric properties, contrary to what previous results reported. The study by DSC and HTXRD didn't evidence for any phase transition in the range

100 K – 923 K. The diffuse phase transition previously reported at 662 K (425 °C) and assigned to ferroelectric-paraelectric phase transition was not detected. The dielectric study of NBZ evidenced a relaxor behavior below room temperature (150 - 250K). The study of this relaxation process revealed an activation energy of 0.17 eV with attempt frequency f_0 = 6.8 10^{11} Hz. The appearance of this relaxation process is similar to the one observed in $BaTiO_3$ based solid-solutions and can be attributed to some cationic disorder due to the mixed occupancy of the A-site of the perovskite lattice by both Na^+ and Bi^{3+} ions. Because of the absence of phase transition, the relative permittivity of NBZ appears noticeably stable since a change of only -2.% for -55°C / 218 K and +5.3% for 85°C / 358K was measured compared to 25°C / 298 K value. Even if the relative permittivity is not very high (ε_r = 80.6 for 1 kHz), this compound appears thus as promising for the elaboration of capacitors requiring high thermal stability of their properties.

Acknowledgments: J. Lelievre wants to thanks the “Region Limousin” which granted its thesis scholarship and the Laboratoire Léon Brillouin, Orsay, France (LLB) for beam time and help in neutron diffraction experiments.

References

[1] M. Demartin Maeder, D. Damjanovic, N. Setter, J. Electroceram. 13 (2004), 385-395
[2] S. Zhang, R. Xia & Thomas R. Shrout, J. Electroceram. 19 (2007), 251-257
[3] T. Takenaka, H. Nagata, Y. Hiruma, Y. Yoshii, K. Matumoto, J. Electroceram. 19 (2007), 259-265
[4] J. Rodel, W. Jo, K. T. P. Seifert, E. Anton, T. Granzow, J. Am. Ceram. Soc. 92 (2009) 1153-1177
[5] R.K. Panda, J. Mater. Sci. 44 (2009) 5049-5062
[6] S.O. Leontwev, R.E. Eitel, Sci. Technol. Adv. Mater. 11 (2010) 044302
[7] J. Rodel, K.G. Webber, R. Dittmer, W. Jo, M. Kimura, D. Damjanovic, J. Europ. Ceram. Soc. 35 (2015), 1659-1681
[8] M. H. Lee, D.J. Kim, J.S. Park, S. W. Kim, T.K. Song, M. Kim, W. Kim, D. Do, I. Jeong, Adv. Mater. 27 (2015), 6976-6982
[9] P.K. Panda, B. Sahoo, Ferroelectrics 474 (2015), 128-143
[10] M. Acosta, N. Novak, V. Rojas, S. Patel, R. Vaish, J. Koruza, G.A. Rossetti, J. Rodel, Appl. Phys. Rev. 4 (2017), 041305
[11] G.A. Smolenskii & al., Izvestiya Akdemii Nauk, Seriya Fizicheskaya, XXXI (1967), 1164-1167 (in Russian)
[12] Y. Yamada, T. Akutsu, H. Asada, K. Nozawa, S. Hachiga, T. Kurosaki, O. Itagawa, H. Fujili, K. Hozumi, T. Kawamura, T. Amakawa, K. Hirota, T. Ikeda, Jpn. J. Appl. Phys. 34 (1995), 5462-5466
[13] L.K. Kumari, K. Prasad, K. L. Yadav, J. Mater. Sci. 42 (2007), 6252-6259
[14] K. Prasad, L.K. Kumari, K.L. Yadav, J. Phys. Chem. Solids 68 (2007), 1508-1514
[15] P. Jaiban, A. Rakachom, S. Bunthzam, S. Jansirisomboon, A. Watcharapasorn, Mater. Sci. Forum 695 (2011), 49-52
[16] P. Jaiban, S. Jansirisomboon, A. Watcharapasorn, ScienceAsia 37 (2011), 256-261
[17] P. Jaiban, S. Jansirisomboon, A. Watcharapasorn, R. Yimnirun, R. Guo, A.S. Bhalla, Ceram. Int. 39 (2013), S81-S85
[18] J.F. Scott, J. Phys.: Condens. Matter **20** (2008) 021001
[19] P. Jaiban, A. Rakachom, S. Jansirisomboon, A. Watcharapasorn, Nanoscale Res. Lett. 7 (2012), 45
[20] A. Rakachom, S. Jansirisomboon, A. Watcharapasorn, Ceram. Int. 39 (2013), S139-S143
[21] B.K. Barick, R.N.P. Choudhary, D.K. Pradhan, Ceram. Int. 39 (2013), 5695-5704
[22] P.E.R. Blanchard, S. Liu, B.J. Kennedy, C.D. Ling, Z. Zhang, M. Avdeev, L. Jang, J. Lee, C. Pao, J. Chen, Dalton. Trans. 43 (2014), 17358-174365
[23] M. Bengagi, F. Morini, M. El Maaoui, P. Marchet, Phys. Status Solidi A, 209 (2012), 2063-2072
[24] V. Petricek, M. Dusek, L. Palatinus, Z. Kristallogr. 229 (2014) 345-352
[25] T.J. Bastow, M.E. Hobday, M.E. Smith, H.J. Whitfield, Solid State Nucl. Mag. 3 (1994), 49-57
[26] R.J. Hill, L.M.D. Cranswick, J. Appl. Crystallogr. 27 (1994), 802-844
[27] A.M. Glazer, Acta Crystallogr. B 28 (1972), 3384-3392
[28] A.M. Glazer, Acta Crystallogr. A 31 (1975), 756-762
[29] C.J. Howards, H.T. Stokes, Acta Crystallogr. B 54 (1998), 782-789.
[30] P.M. Woodward, Acta Crystallogr. B 53 (1997), 32-43

[31] C.J. Howard, T. Stokes, Acta Crystallogr. B 54 (1998), 782-789
[32] A. A. Belik, Matsuhita, M. Tanaka, E. Takayama-Muromachi, Inorg. Chem. 52 (2013) 12005-12011
[33] M. Groting, S. Hayn, K. Albe, J. Solid State Chem. 184 (2011) 2041-2046
[34] E. Aksel, J.S. Forrester, J.C. Nino, K. Page, D.P. Shoemaker, J.L. Jones, Phys. Rev. B 87 (2013) 104113
[35] K. Datta, R.B. Neder, A. Richter, M. Gobbels, J. C. Neuefeind, B. Mihailova, Phys. Rev. B 97 (2018) 184101
[36] H. Ogihara, C.A. Randall, S. Trolier-McKinstry, J. Am. Ceram. Soc. 92 (2009) 110-118
[37] S.S.N. Bharadwaja, J.R. Kim, H. Ogihara, L.E. Cross, S. Trolier-McKinstry, C.A. Randall, Phys. Rev. B 83 (2011) 024106
[38] L. Wu, X. Wang, Z. Shen, L. Li, J. Am. Ceram. Soc. 100 (2017) 265-275
[39] V. Dorcet, P. Marchet, G. Trolliard, J. Europ. Ceram. Soc. 27 (2007) 4371-4374

Figure Caption

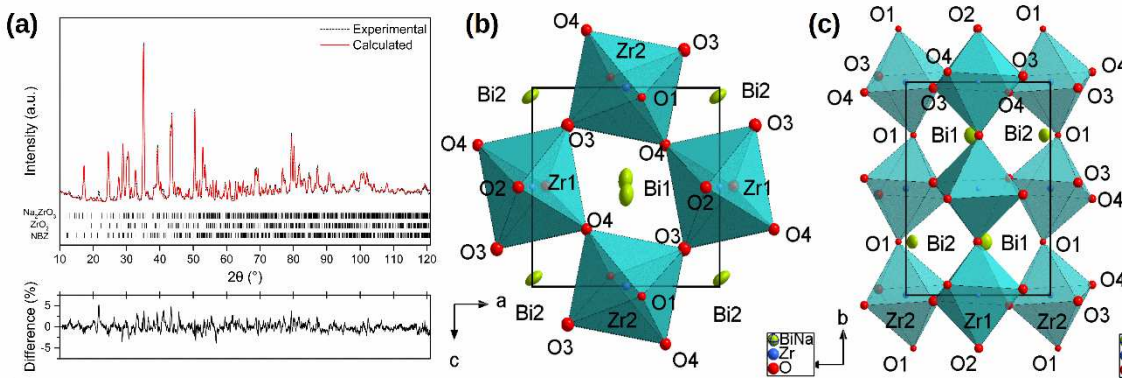

Fig. 1: (a) Room temperature neutron diffraction pattern of NBZ powder and results of crystallographic refinement using the space group $P2_1/m$ (SG #11) and taking into account secondary phases Na_2ZrO_3 and ZrO_2 and representation of the obtained NBZ structure along the directions (b) [010] and (c) [100]

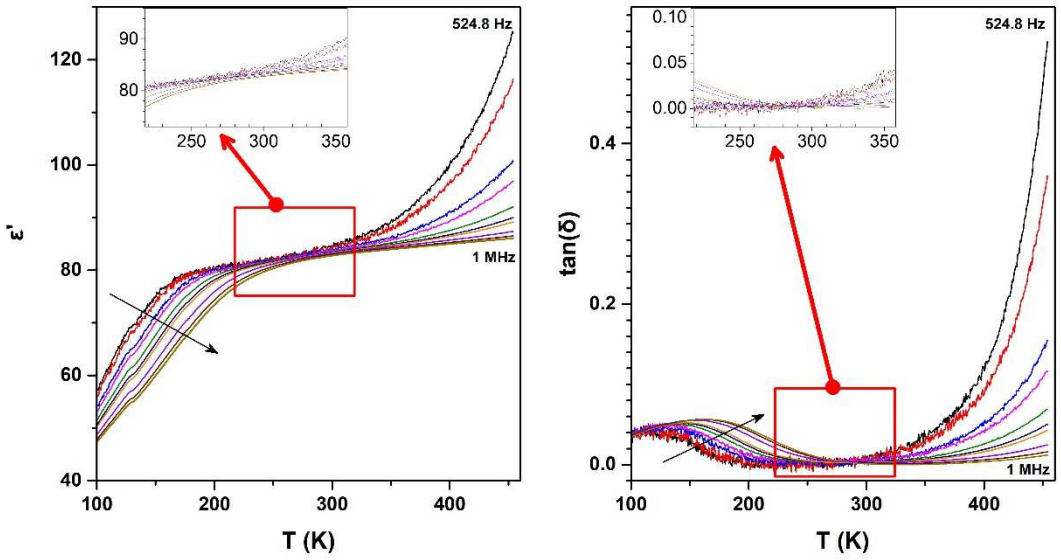

Figure 2 : Evolution of (a) the relative permittivity and (b) the dielectric losses tan(δ) of NBZ as a function of the temperature for different frequencies (524.8 Hz, 1 kHz, 5.25 kHz, 10 kHz, 33.1 kHz, 69.2 kHz, 100 kHz, 331.1 kHz, 691.8 kHz and 1 MHz). The arrows indicate increasing frequencies. The details correspond to the range -55 °C / 218 K – 85 °C / 358 K (EIA standard for temperatures).

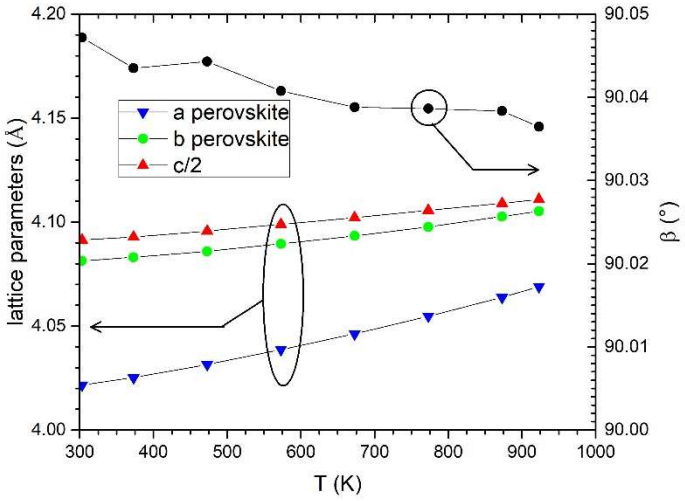

Figure 3 : Thermal evolution of the lattice parameters and of the β monoclinic angle of NBZ from room temperature 303 K (30°C) to 923 K (650°C) as determined by HTXRD ($a_p = a_m/\sqrt{2}$, $b_p = b_m/\sqrt{2}$, $c_p = c_m/2$).

Supplementary materials

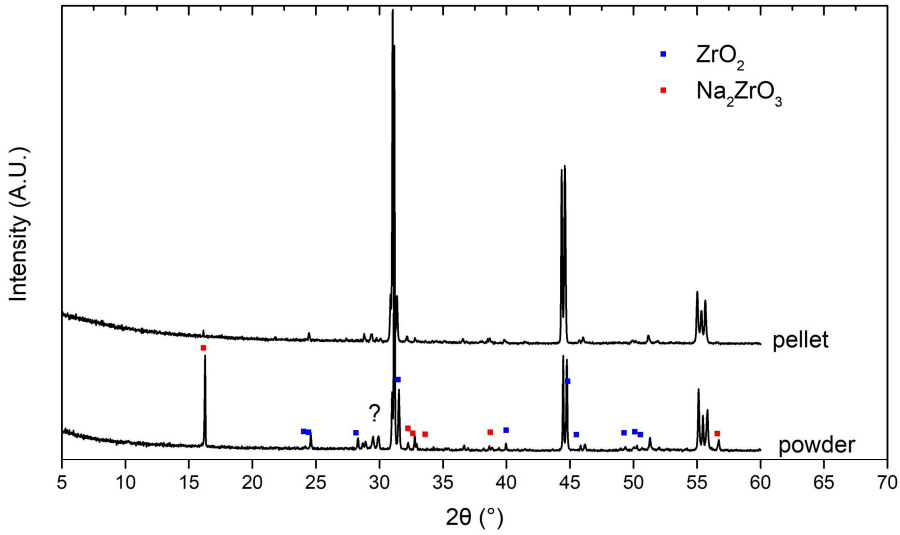

Fig. S1: XRD pattern of NBZ powders and sintered pellet.

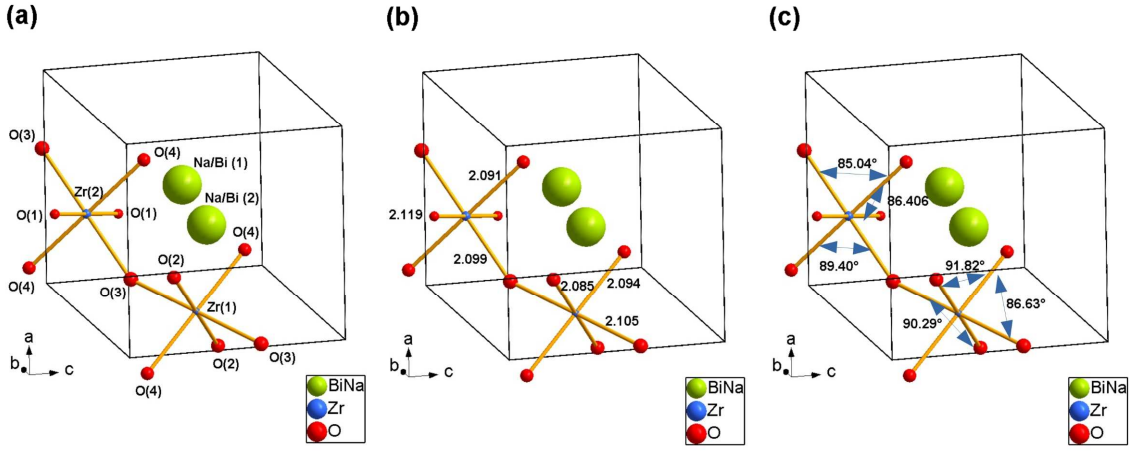

Fig. S2: Distance and angles in NBZ as determined by structural refinement.

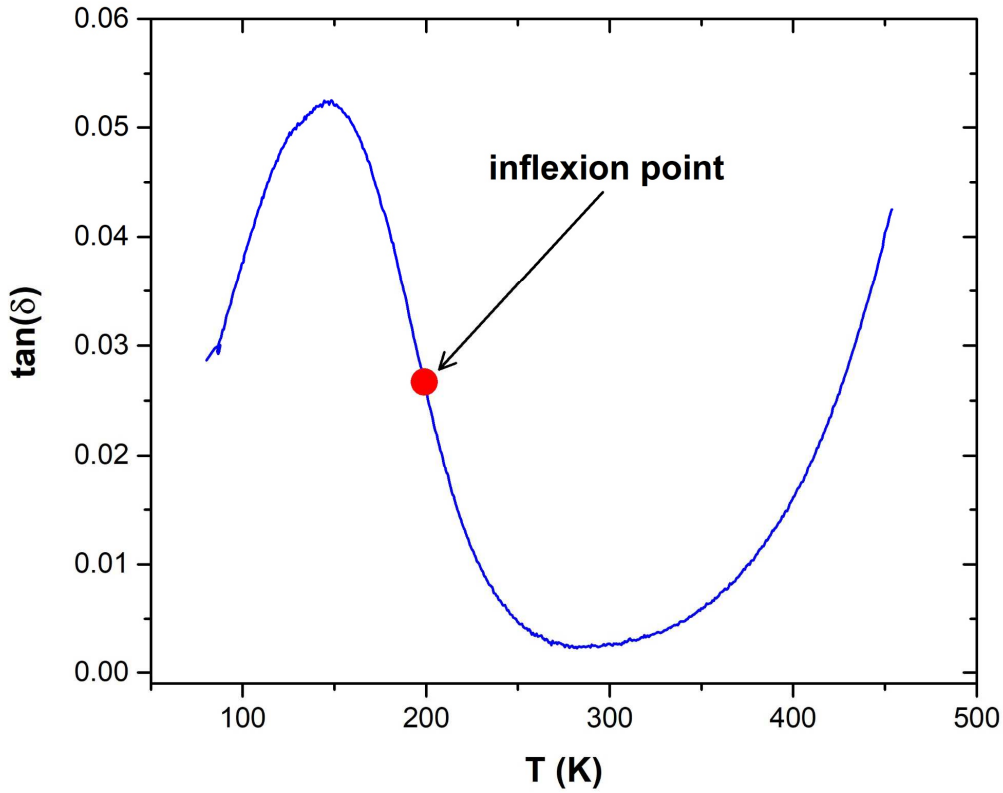

Fig. S3: Determination of the temperature of inflexion point of tan(delta) curve.

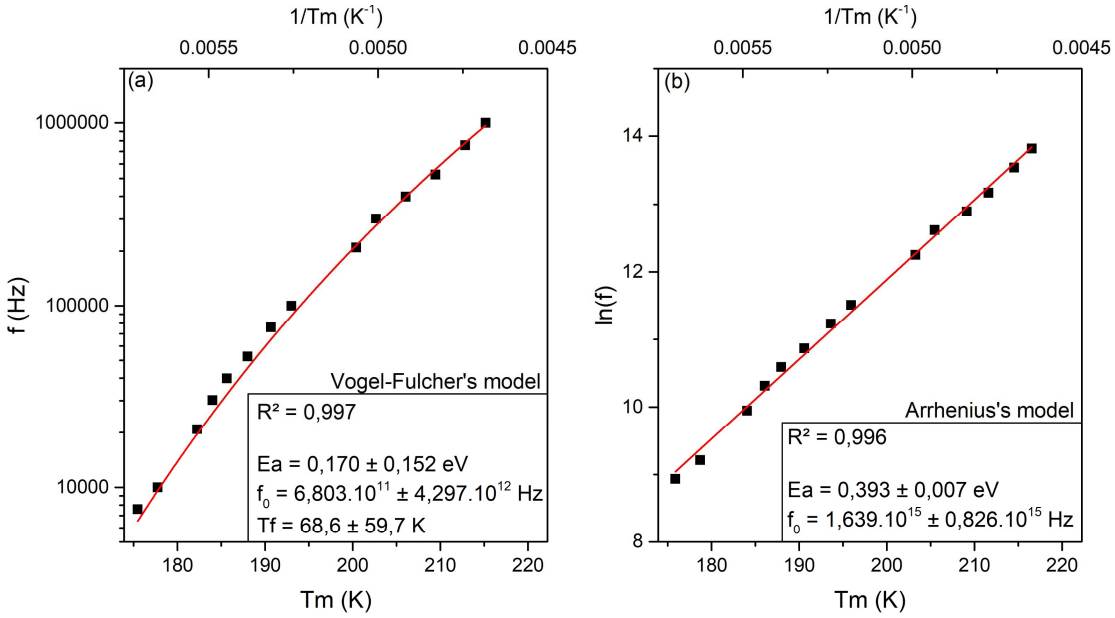

Fig. S4: Vogel-Fulcher and Arrhenius fitting of permittivity curves.

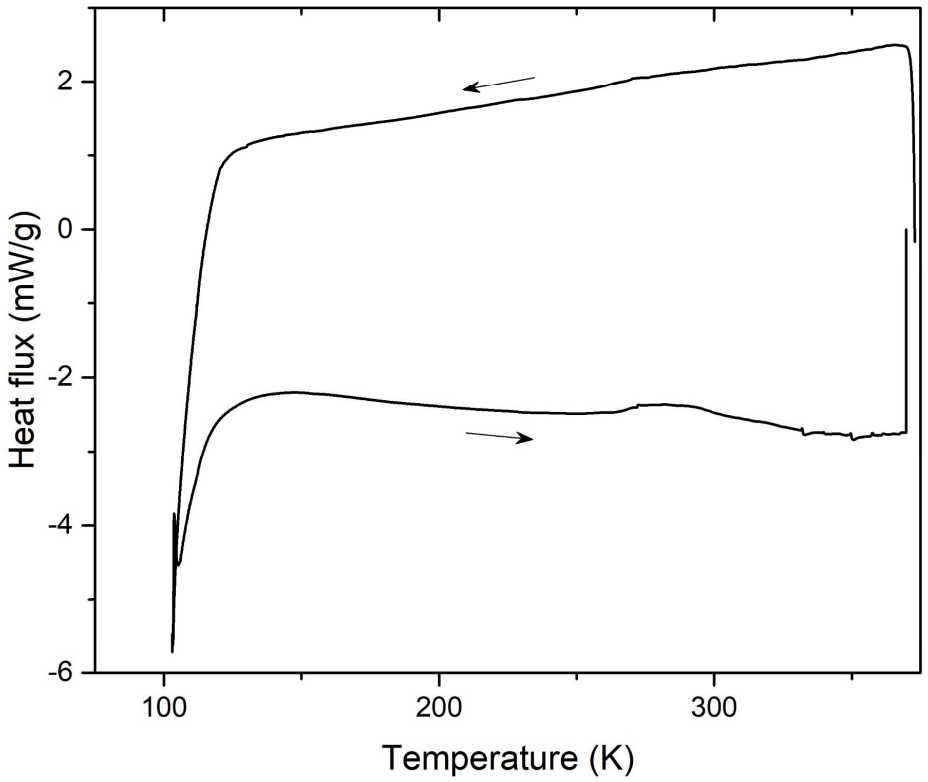

Fig. S5: Low temperature DSC curves.

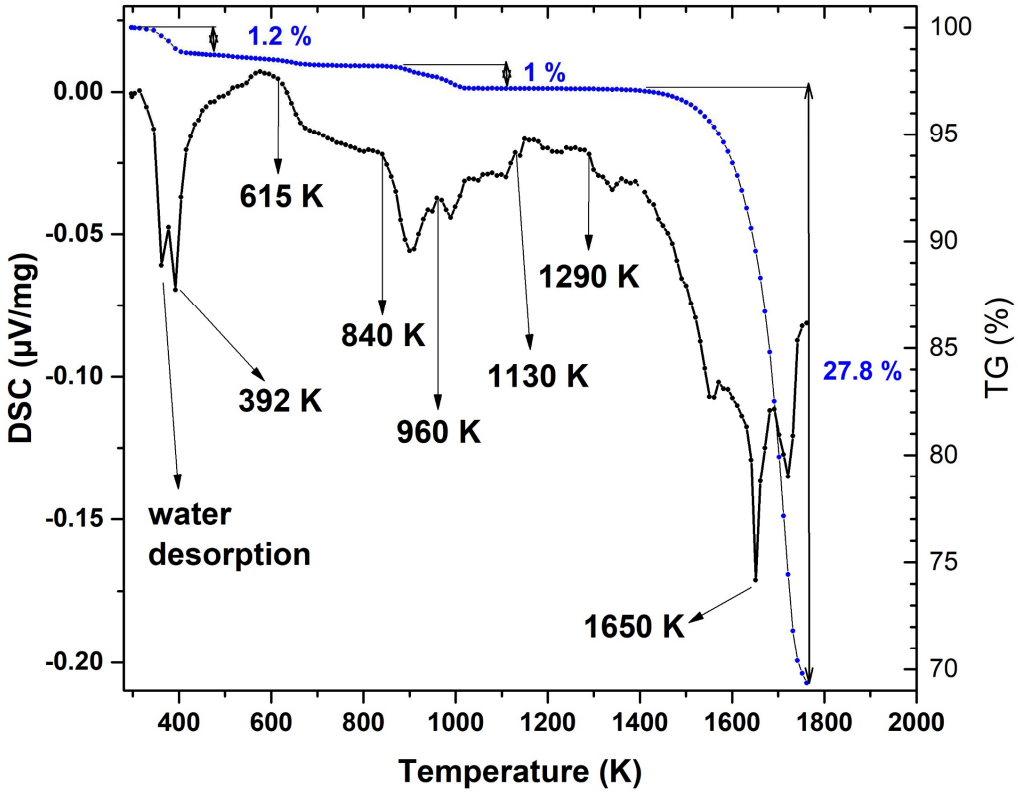

Fig. S6: High temperature DSC curves.

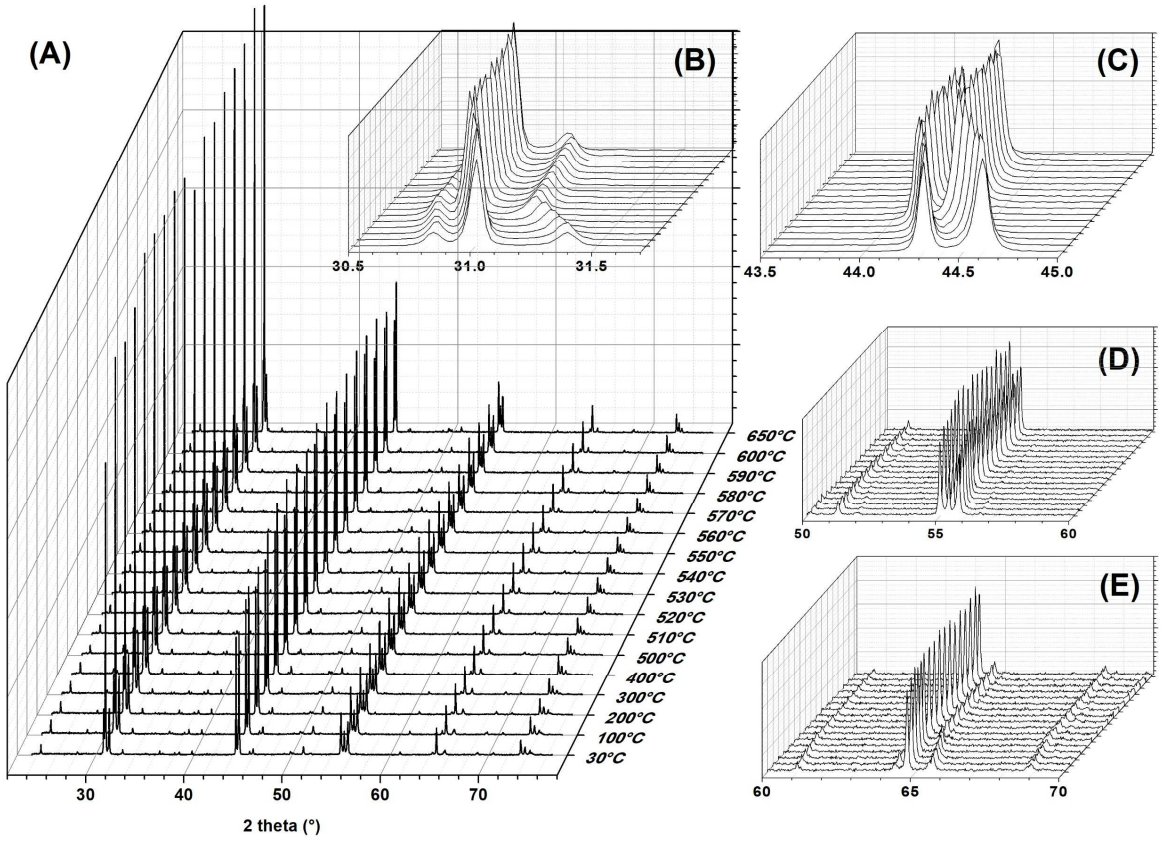

Fig. S7: temperature programmed XRD patterns of NBZ compound.